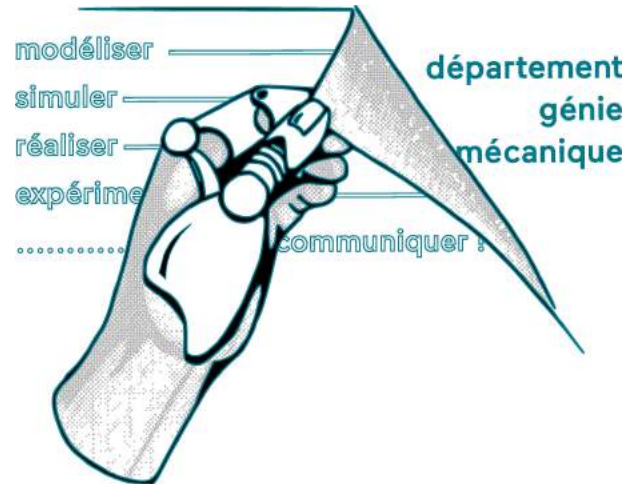
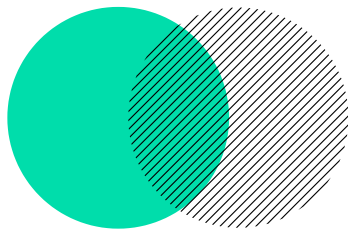
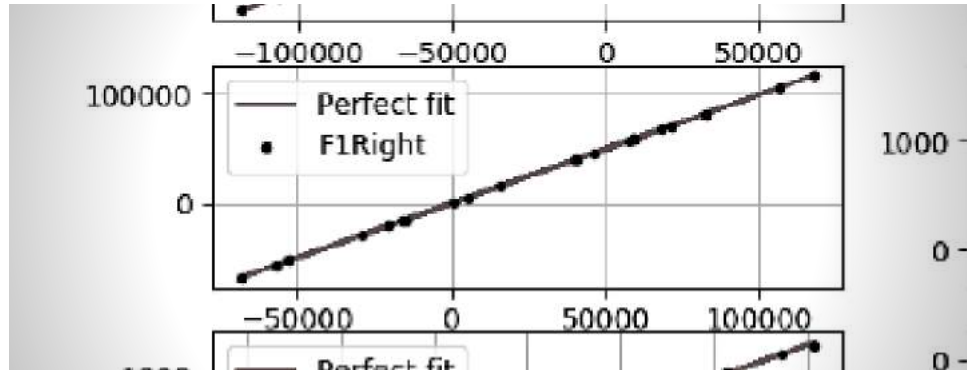
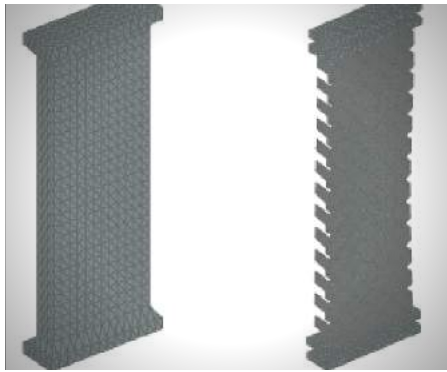
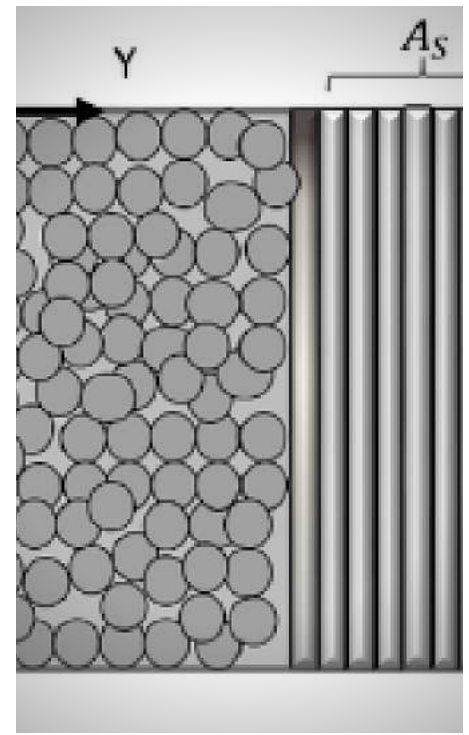


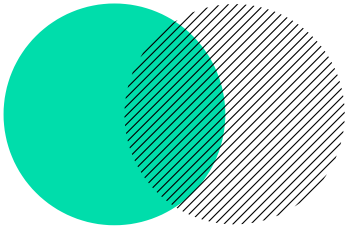
$$\left\{ \begin{aligned} M &= \sum_{i \in A} \frac{Z_i - b_i}{G_i} - m_p \\ x &= \frac{\left( \sum_{i \in A} \left( \frac{Z_i - b_i}{G_i} \right) x_i \right) - m_p x_p}{\left( \sum_{i \in A} \frac{Z_i - b_i}{G_i} \right) - m_p} \\ y &= \frac{\left( \sum_{i \in A} \left( \frac{Z_i - b_i}{G_i} \right) y_i \right) - m_p y_p}{\left( \sum_{i \in A} \frac{Z_i - b_i}{G_i} \right) - m_p} \end{aligned} \right.$$



# RESEARCH PROJECTS

STUDENTS OF THE DEPARTMENT OF MECHANICAL ENGINEERING

20  
20  
21



# MONITORING AND FORECASTING OF FAULTS FOR THE POWDER BED LASER FUSION PROCESS BY IMAGE ANALYSIS AND IN- PROCESS MEASUREMENT

---

**A. BLONDIN - A. HILZHEBER**  
***Y. QUINSAT - N. MULLER***

TER M1 2020-2021  
FINAL DEFENSE OF RESEARCH PROJECTS  
13 April 2021, Gif-Sur-Yvette, France

école —————  
normale —————  
supérieure —————  
paris – saclay ———

# Monitoring and forecasting of faults for the powder bed laser fusion process by image analysis and in-process measurement

A. Blondin <sup>\*</sup>, A. Hilzheber<sup>†</sup>, Y. Quinsat<sup>♡</sup> and N. Muller<sup>◇</sup>

<sup>\*</sup> Mechanical engineering department  
Ecole Normale Supérieure Paris Saclay  
*4 avenue des Sciences, 91190 Gif-Sur-Yvette, France*  
e-mail: aureore.blondin@ens-paris-saclay.fr

<sup>†</sup> Mechanical engineering department  
Ecole Normale Supérieure Paris Saclay  
*4 avenue des Sciences, 91190 Gif-Sur-Yvette, France*  
e-mail: antonin.hilzheber@ens-paris-saclay.fr

<sup>♡</sup> Laboratoire universitaire de recherche en production automatisé  
Ecole Normale Supérieure Paris Saclay  
*4 avenue des Sciences, 91190 Gif-Sur-Yvette, France*  
e-mail: yann.quinsat@ens-paris-saclay.fr

<sup>◇</sup> Laboratoire universitaire de recherche en production automatisé  
Ecole Normale Supérieure Paris Saclay  
*4 avenue des Sciences, 91190 Gif-Sur-Yvette, France*  
e-mail: nicolas.muller@ens-paris-saclay.fr

**KEYWORDS:** Laser Powder Bed Fusion; porosity; layer thickness.

## ABSTRACT

### General Information

Additive Manufacturing, more precisely the Laser Powder Bed Fusion technology, is increasingly used for its ability to build complex pieces. However, this process is hard to master and obtain high-quality pieces. It is common to encounter issues on material integrity, such as porosity inside parts[1]. These issues could be explained by incorrect management of the different parameters on LPBF machines[2], which determine the volumetric energy density. Previous researches have described methods[1] to detect layering defects, such as embedded vision systems[3], which automatically detect powder spreading irregularities. These defects could be regarded as a disruption of layer thickness. However, no study has evaluated the influence of these anomalies on material integrity. A better comprehension of their role on material integrity is required to adjust the layer thickness during fabrication. Thus, it will help to reduce the porosity and increase parts quality.

## Method and results

We performed an experimental plan to characterize the impact of the layer thickness on the porosity. We tested different thicknesses with nine pieces with a variation of layer thickness, one different speed, power each. After having printed these pieces, we performed a micrograph study to analyze the inside material. We took three micrographs for every parameter set, 108 in total. Then, we used them to determine the distribution of porosity using Matlab.

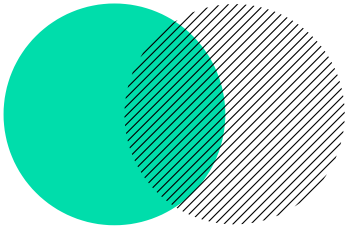
We classified the different types of porosities in relation to the parameter sets. An Anonvan study indicated that layer thickness irregularities are likely to lead to porosities. Consequently, issues on powder spreading could create material health problems.

## Conclusion

Thanks to our study, the monitoring and forecasting of faults for the powder bed laser fusion process are relevant and interesting, to increase part quality. Moreover, further experimentations could be done, to test other parameter sets. Then we would be able to verify the significant influence of layer thickness on the apparition of the different porosity types.

## REFERENCES

- [1] L.Scimea, D.Siddelb , S.Bairdc , V.Paquita. Layer-wise anomaly detection and classification for powder bed additive manufacturing processes: A machine-agnostic algorithm for real-time pixelwise semantic segmentation. *Additive Manufacturing* **Vol:36**, 2020.
- [2] F.Iman, A.Gaikwad, M.Montazeri, P.Rao1, H.Yang , E.Reutzel. Process Mapping and In-Process Monitoring of Porosity in Laser Powder Bed Fusion Using Layerwise Optical Imaging. *Transactions of the ASME* **Vol:140**, 2018.
- [3] B. K. Foster, E. W. Reutzell, A.R. Nassar, B. T. Hall, S.W. Brown, C.J. Dickman.Optical, layerwise monitoring of powder bed fusion



(a)

# EXPERIMENTAL STUDY OF THE BUCKLING OF ARCHITECTURED MATERIALS UNDER BIAXIAL COMPRESSION

---

**T. JACQUET - J. FAVRE**

TER M1 2020-2021  
FINAL DEFENSE OF RESEARCH PROJECTS  
13 April 2021, Gif-Sur-Yvette, France

école \_\_\_\_\_  
normale \_\_\_\_\_  
supérieure \_\_\_\_\_  
paris-saclay \_\_\_\_\_

# Experimental study of the buckling of architected materials under biaxial compression

Thomas JACQUET\*, Justin FAVRE†

\*† Mechanical Engineering Department  
École Normale Supérieure Paris-Saclay  
4 Avenue des Sciences, 91190 Gif-sur-Yvette

\* e-mail: thomas.jacquet@ens-paris-saclay.fr and † e-mail: justin.favre@ens-paris-saclay.fr

**KEYWORDS:** Architected materials; biaxial compression; buckling; test machine.

## ABSTRACT

### 1 General context

Because of their particular internal structures combining matter and void, architected materials can have enhanced intrinsic properties (e.g. stiffness anisotropy or specific yield stress) that bulk materials can't. Such materials present these uncommon behaviors because of their cell structures, made of slender beams or walls. Under load, those cells tend to buckle (see Figure 1).

The goal of this research project is to design and build a biaxial crushing test machine, in order to confront C. Combescure [2] numerical model of a honeycombed architected material under biaxial crushing with experiments. Other researchers, like S.D. Papka and S. Kyriakides [1] or S. Shan et al. [3], also worked on biaxial crushing test machines, yet, their machines did not allow measurements of the stress applied to the sample. C. Fredy [4] did include a measure of the normal forces applied to each side of the sample, but the torques and tangential forces are yet to be measured.

### 2 Our project

Technically speaking, our project is to design a machine adapted to specimen size up to  $180 \times 180 \text{ mm}^2$ , compaction ratios up to 50% and with enough force capacity to crush ABS honeycombs. Its main feature of interest is that it will allow the measurement of all the in-plane force components on each side of the sample.

The first step is to find a machine structure enabling high crushing ratio and measurement of the forces applied to the sample. The crushing plates stand on a whole system of moving parts, using linear bearings. The system is set in motion by 4 stepper motors based linear actuators. To be reliable, the measuring system had to be as close as possible to the sample because of the forces transiting through the machine, and not exclusively through the sample. The measuring system is made of  $4 \times 3$  load cells that are organized in such a way they give the searched in-plane force components. The expected force uncertainty

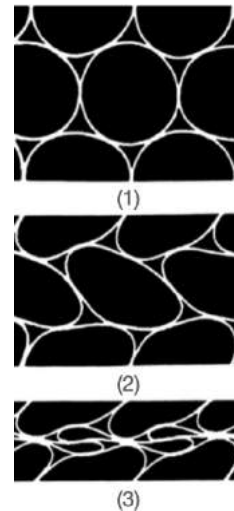


**Figure 1:** Buckling of circular cells (from [1])

is around 0.1 kg (on a scale from 0 to 20 kg). However, the uncertainty of the applied displacement is significant because of the stiffness of the machine, but more accurate measures will be obtained by kinematic full-field techniques.

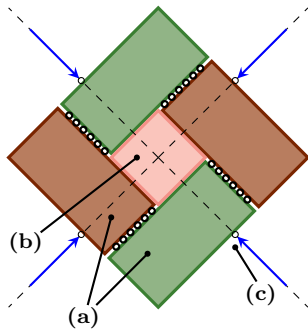


**Figure 2:** Principle of the machine:  
(a) crushing part; (b) sample; (c) displacement application point

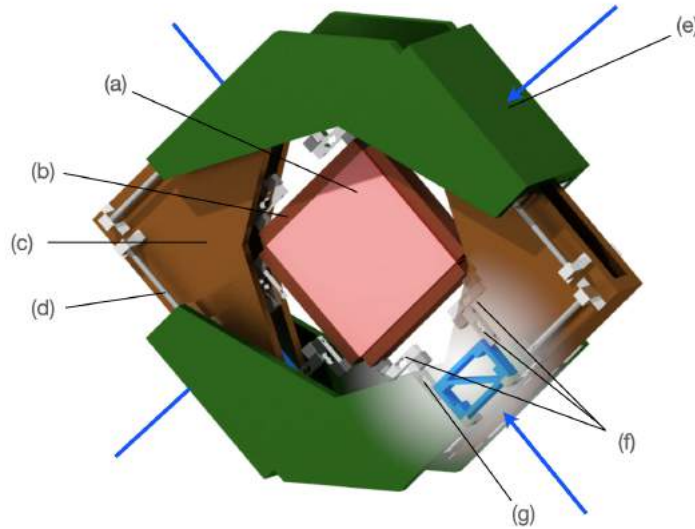


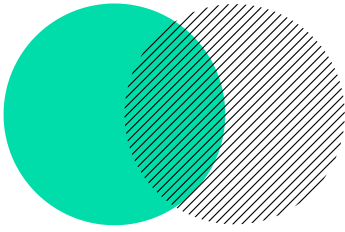
**Figure 3:** CAD of machine:  
(a) sample; (b) pressure plate; (c) crushing part; (d) linear bearing; (e) displacement application point; (f) load cell; (g) compliant cell

The second step was to manufacture it. We decided to use plywood for its low weight and price and high machinability. Its stiffness is sufficient for our range of loads. We also thought we could rely on its precise width to assemble all the parts of the machine together, but it turns out to be wrong, inducing unexpected time loss.

The last step will consist of conducting a biaxial crushing test on the sample C. Combescure used for her numerical model [2], in order to validate or invalidate it.

## REFERENCES

- [1] S.D. Papka, S. Kyriakides. Biaxial crushing of honeycombs - Part I: Experiments. *Int. J. of Solids and Structures* **36(29)**:4367-4396, 1999.
- [2] C. Combescure, P. Henry, R.S. Elliott. Post-bifurcation and stability of a finitely strained hexagonal honeycomb subjected to equi-biaxial in-plane loading. *Int. J. of Solids and Structures* **88(89)**:296-318, 2016.
- [3] S. Shan et al. Harnessing Multiple Folding Mechanisms in Soft Periodic Structures for Tunable Control of Elastic Waves. *Adv. Funct. Mater.* **24(31)**:4935-4942, 2014.
- [4] C. Fredy, *Modeling of the mechanical behavior of polytetrafluoroethylene (PTFE) compounds during their compaction at room temperature*. PhD Thesis, Univ. Pierre et Marie Curie - Paris VI, 2015.



# REPRESENTING MODELS IN SOLID MECHANICS USING NEURAL NETWORKS

---

**T. NANICHE - S. TOURAIVANE**  
***E. BARANGER***

TER M1 2020-2021  
FINAL DEFENSE OF RESEARCH PROJECTS  
13 April 2021, Gif-Sur-Yvette, France

école —————  
normale —————  
supérieure —————  
paris — saclay —————

# Representing Models in Solid Mechanics using Neural Networks

T. Naniche\*, S. Touraivane†, E. Baranger◇,  
Département de Génie Mécanique, ENS Paris-Saclay, 4 Avenue des Sciences,  
91190 Gif sur Yvette, France

\* e-mail: theo.naniche@ens-paris-saclay.fr

† e-mail: shangaya.touraivane@ens-paris-saclay.fr

◇ e-mail: emmanuel.baranger@lmt.ens-cachan.fr

**KEYWORDS:** Neural Networks; Solid Mechanics; Lagrangian Mechanics.

## ABSTRACT

### Context and introduction

Over the past few decades, neural networks have become one of the most promising and studied tools in several fields. While their use in fields such as image processing is well known and understood, their applications in mechanics are still in their early development.

Most of the applications of neural networks in mechanics are mere interpolations of the motion of complex systems. In those cases, the neural network takes a set of parameters describing the system as an entry and returns an approximation of the motion function of the structure, relying on Cybenko's theorem to ensure the precision of its interpolation.[1]

The main issue with this approach is that the network is trained to predict the behaviour of the system on a restricted operating range and can never be expected to extrapolate the behaviour correctly out of this range. Moreover, this method does not ensure the physical plausibility of the predictions.[2]

Our work aims at using neural networks in a way that allows to implement physical properties in order to ensure the plausibility of its predictions.

### Methods

To implement physical properties into neural networks, we decided to focus on two issues. The first one was to study Lagrangian and Hamiltonian mechanics to understand what properties could be used and how we could implement them.[3] The second one was to get a better understanding of deep neural networks.

This study led us to the idea that theoretical models based on Lagrangian mechanics could be used to calculate the error of the prediction of a neural network instead of using measured data.[2] For instance, for a neural network predicting the stiffness of a spring in a mass-spring system, the idea would be to compute the theoretical motion of the system from the approximated stiffness to compare it with the measured motion used as an entry instead of comparing the computed stiffness to a measure of the real one.

One of the keys to correctly implement such a method is to be able to describe the motion of the structure with the predicted stiffness from a numerical calculus in a way that ensures physical plausibility. To avoid numerical dissipation of the energy in the motion, we implemented symplectic integrators to calculate the generalized coordinate  $q$  and conjugate momenta  $p$  of the spring-mass system.[4]

We chose to write our codes using Keras and Tensorflow, two common Python libraries in machine learning. To take into account the physical properties of our system, we identified two options; creating our own loss function or creating a non-trainable last layer in the neural network. However, we rapidly realised that implementing our own loss function would violate certain rules of the Keras syntax. In order to overcome this problem, we decided to create a customized layer that would allow us to use the built-in back-propagation method of Keras.

## Key results and interpretations

We developed such a neural network and made it learn how to recognize the stiffness and mass of the system with only a set of position and speed as an entry.

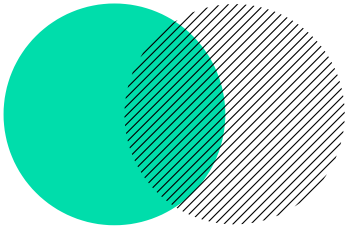
However, We found that our method needed a long time to converge to its final solution. In addition, we observed that the problem we were trying to solve had a lot of local minima that are difficult to avoid. In order to deal with this last problem, we tried to use the adaptive learning rate algorithm built in tensorflow with no significant improvement yet. Another idea to overcome this issue would be to address the problem from a frequential point of view instead of a temporal one since the mass and stiffness of a mass-spring system are directly linked to its pulsation.

Working on the initialisation of the network could be an interesting idea too. Indeed, to avoid local minima, finding an initialisation close to the global minimum is a common solution.

Lastly we could try to investigate the importance of the structure of the network. The number of neurons on consecutive layers and the deepness of the network both have an effect on the convergence speed and we did not try to use this to its full potential.[5]

## REFERENCES

- [1] G. Cybenko. Approximation by superposition of a sigmoidal function. *Mathematics of Control, Signals and Systems* **Vol:303-314**, 1989.
- [2] M. Lutter, C. Ritter, J. Peters. Deep Lagrangian Networks: Using Physics as Model Prior for Deep Learning. *Journal Title* **Vol:Pages**, 2019.
- [3] L.D. Landau, E.M. Lifshitz. *Mechanics: Volume 1. Elsevier*. Elsevier, 1982.
- [4] E. Hairer. Lecture 2: Symplectic integrators. *Geometric Numerical Integration*, 2010.
- [5] L. Arnold, H. Paugram-Moisy, M. Sebag. Optimisation de la Topologie pour les Réseaux de Neurones Profonds. In: *17e congrès francophone AFRIF-AFIA Reconnaissance des Formes et Intelligences Artificielles*, Caen, France, Jan 2010.



# STRATEGY FOR THE DIMENSIONING OF STRUCTURES BY A LOCAL-GLOBAL NON- INTRUSIVE APPROACH

---

**J. RUEL - R. THEVENOT**

TER M1 2020-2021  
FINAL DEFENSE OF RESEARCH PROJECTS  
13 April 2021, Gif-Sur-Yvette, France

école —————  
normale —————  
supérieure —————  
paris — saclay ———

# Strategy for the dimensioning of structures by a local-global non-intrusive approach

Jean RUEL\*, Raphaël THÉVENOT†

\* † Département de génie mécanique  
École Normale Supérieure Paris-Saclay  
4, avenue des Sciences 91190 Gif-sur-Yvette  
e-mail: \* jean.ruel@ens-paris-saclay.fr ; † raphael.thevenot@ens-paris-saclay.fr

Supervised by Olivier Allix, Pierre Gosselet, Stéphane Guinard

**KEYWORDS:** design strategy; local-global non intrusive approach; surrogate model.

## ABSTRACT

### General Information

During the design phase, a product is designed in broad outline and then iteratively, finer and finer details are inserted and studied. This approach is called a top - down approach. This approach is in particular conditioned by calculation practices. For cost reasons, global models and local models (level of fine detail) are simulated separately. As a result, this process is long, costly and poorly effective because there is no interaction between the different scales of the structure. In this context, and in order to reduce design time, local/global coupling methods have been developed [1, 2]. These methods allow, thanks to an iterative calculation, to take into account the different levels of detail of a structure. Thus, they make it possible to adapt calculation practices to design practices. In this way, different local models could be integrated and tested at an early stage of design. This work proposes a design strategy using local-global approaches. We will focus on the construction of a surrogate model of the local model [3], always with the aim of reducing calculation times. The method will be illustrated on a simplistic but representative design case.

### Methodology

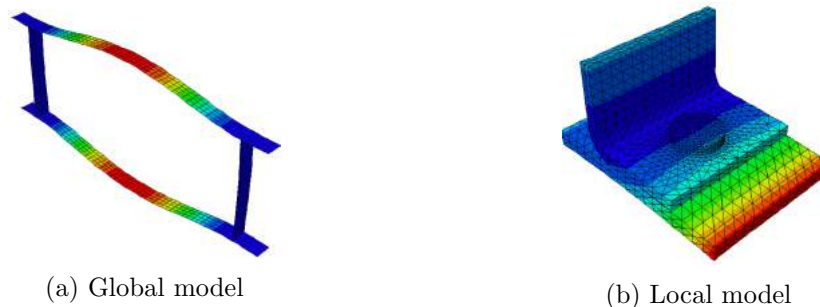


Figure 1: Study case

The design case selected in this study is presented in Figure 1. The global system is a 2D simulation of an internal wing box and the local system is a 3D simulation of a bolted joint. A first step to create a surrogate model was to decide the design parameters and the response of the surrogate model. The design parameters chosen were different geometry sets (several geometric parameters being linked) and the preload of the bolt as inputs and a local criteria (the maximum of the Von Mises stress) as output. The behavior selected was to associate each interface surface to a rigid body with planar movement, this simplification reduced the number of degree of freedom to 3 for each interface (2 translations and 1 rotation). For this

project, the surrogate model was separated in two parts: a dynamic part linking displacement to stress with a behavior model and a second part useful for designing process which compute the maximum Von Mises stress. Two different models were tested to identify a behavior model, a first one linear and a second one based on polynomial regression. The linear model is equivalent to find a matrix linking the vector of inputs to the vector of outputs, thus it was determined by evaluating the matrix on a base of the input space. The regression model was computed on a known database of the local system.

## Results

The evaluation of the model on a one-to-one basis proved to be unwise and too inaccurate. The regression method is more suitable. The lowest error is obtained by polynomial regression of order 2 and 3. One way to evaluate the results of different surrogate models is to plot a graph with each point represents the couple  $(F_{3D\ Simulation}^i, F_{Surrogate}^i)$ , for a perfect surrogate model all points would be on the line  $y=x$  (see figure 2).

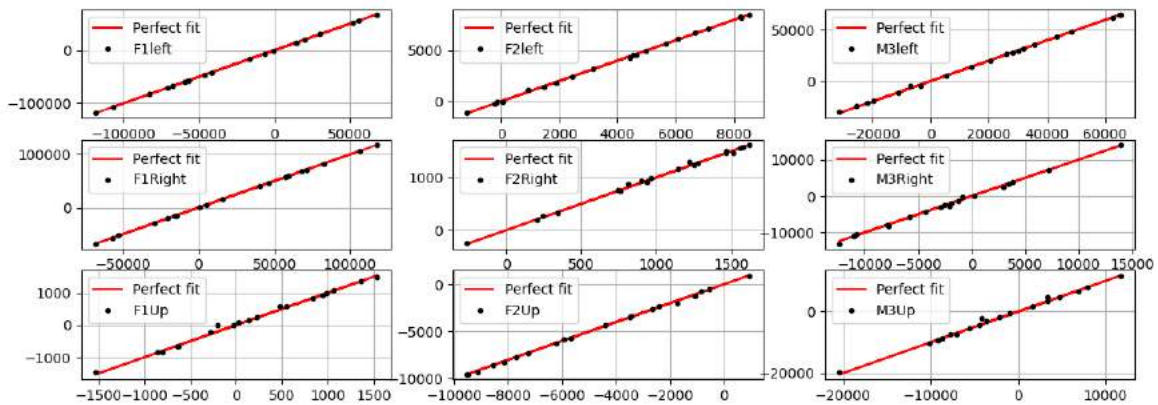


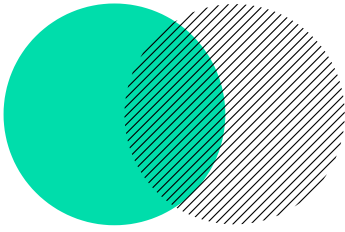
Figure 2: Comparison between a regression model of degree 3 and the 3D simulation results. Each figure represents one generalized effort (F1, F2, M3) for each interface (Up, Right, Left).

## Conclusion and future work

Results show that a surrogate model can be a good alternative to the time-consuming 3D simulation with a minimum of errors. Further work may focus on the adaptation of the non-intrusive global-local method when the local model is replaced by a surrogate model. On the other hand, Abaqus cosimulation tools will have to be adapted in order to provide the engineer with a fast and efficient tool in the design office.

## REFERENCES

- [1] O. Allix, P. Gosselet. Non intrusive Global/local coupling techniques in solids mechanics: an introduction to different coupling strategies and acceleration techniques. *Modeling in Engineering Using Innovative Numerical Methods for Solids and Fluids*, 599, Springer Nature Switzerland AG pp.203-220, 2020.
- [2] L. Gendre, O. Allix, P. Gosselet, F. Comte. Non intrusive and exact global/local for structural problems with local plasticity. *Computational Mechanics*, Springer Verlag, 2009, 44(2), pp.233-245. 10.1007/s00466-009-0372-9 . hal-00437023
- [3] Oberkampf, W. L., M. Pilch and T. G. Trucano (2007), *Predictive Capability Maturity Model for Computational Modeling and Simulation*. Sandia National Laboratories, SAND2007-5948, Albuquerque, NM.



# DEVELOPMENT OF NUMERICAL TOOLS FOR IN-SITU CONTROL OF THE ADDITIVE LPBF MANUFACTURING PROCESS

---

**L. DESHAYES - G. LAGORCE**  
**C. TOURNIER - L. CHAMOIN**

TER M1 2020-2021  
FINAL DEFENSE OF RESEARCH PROJECTS  
13 April 2021, Gif-Sur-Yvette, France

école \_\_\_\_\_  
normale \_\_\_\_\_  
supérieure \_\_\_\_\_  
paris-saclay \_\_\_\_\_

# Development of numerical tools for in-situ control of the additive LPBF manufacturing process

L. Deshayes\*, G. Lagorce\*, C. Tournier<sup>◇</sup>, L. Chamoin<sup>†</sup>

\* Department of Mechanical Engineering  
Ecole normale supérieure Paris-Saclay  
4, avenue des Sciences, 91190 Gif-sur-Yvette, France  
{liam.deshayes ; gwendal.lagorce}@ens-paris-saclay.fr

<sup>◇</sup> Université Paris-Saclay  
Ecole normale supérieure Paris-Saclay  
LURPA  
4, avenue des Sciences, 91190 Gif-sur-Yvette, France  
christophe.tournier@ens-paris-saclay.fr

<sup>†</sup> Université Paris-Saclay  
Ecole normale supérieure Paris-Saclay  
LMT  
4, avenue des Sciences, 91190 Gif-sur-Yvette, France  
ludovic.chamoin@ens-paris-saclay.fr

**KEYWORDS:** Additive Manufacturing; Laser Powder Bed Fusion; Residual Stresses.

## ABSTRACT

### General Context

Additive Manufacturing (AM) has recently become an attractive technology due to its capacity to build complex geometry. However issues regarding consistency and feasibility of the process have been risen. Here we focus on the Laser Powder Bed Fusion (LPBF) process, in which metallic powders are selectively melted by layers with a laser into a solid metallic part. The use of laser creates thermal gradients and during cooling phases material retracts in heterogeneous way, capturing residual stresses. The aim of the present study is to obtain an analytical model of residual stresses based on the laser path and the thermal gradients and to build afterward a scanning strategy basis for in-situ and real-time control of the process in order to reduce residual stresses in the final printed part.

### Methods

To assess a residual stress map, a temperature map of the building part is needed. To do so, a method named FLASH has been previously developed [1]. The thermal effect of the laser trajectory on the powder and the printed part is simulated with an analytical model as a succession of elementary pulses (Figure 1). The pulse moves according to the laser trajectory, which allows reasonable simulation times.

The residual stresses are determined with a one-dimensional model adapted from welding mechanics [2]. In welding mechanics, residual stresses can be calculated with the inherent strain method [2]. The method is based on a thermal elastic-plastic analysis on three bars: two bars representing the two parts welded together and one representing the welded joint.

Previous studies [3 & 4] have applied the inherent strain method to the LPBF process (Figure 2). The model considers two bars, one for the solidified track and one for the exposed track. Based on this model, a code has been developed in order to calculate a stress map by using the thermal map obtained by the FLASH method. The last solidification time of the solidified track is determined by analysing the thermal map.

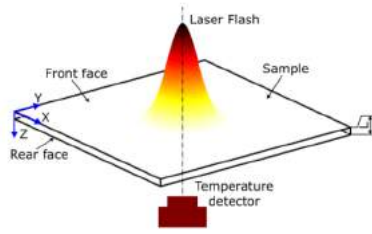


Figure 1: Principle of the FLASH method [1]

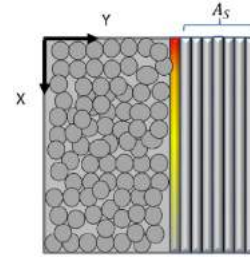


Figure 2: Welding model used for LPBF process [3]

## Results

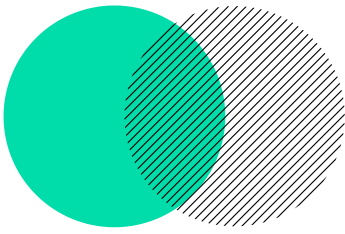
The yield temperature of the track is determined and used to calculate residual stress. At each iteration, that is to say each new track, we assume that only the new weld bead will plastify and perform an elastic-plastic analysis to determine the yield temperature. Thus, residual stresses can be calculated based on this temperature. Depending on the value of the yield temperature, two regimes of plasticity are allowed: one under the yield strength and one equal to the yield strength. The analytical calculation permitted to show that each new weld bead can be considered as the simple case of welding, regardless of the previous beads. This model is fast to compute, due to its computational complexity, which is linear with the number of spatial elements. The residual stresses were determined for both a simple elementary pulse and a whole layer of simple scanning path. Unfortunately, we could not properly validate nor invalidate the model, due to a lack of experimental data. However, the code gives results with an order of magnitude that correspond to literature's results.

## Further work

Work has to be done to generalize the method to a two- or three-dimensional calculation to cover a surface/volume and thus obtain a complete residual stress map. Moreover, further research is also needed to calculate residual stresses in every direction of a plane to be able to assess more complex geometries. Then the challenge is to build a scanning scenario database that would allow the prediction, via interpolation, of the residual stresses in the printed part during the process at each layer and allow a choice of a strategy to reduce residual stresses. Preliminary results of this will be given during the final defence of TER.

## REFERENCES

- [1] K.Ettaieb, S.Lavernhe, C.Tournier, A flash based thermal simulation of scanning paths in LPBF additive manufacturing, *Rapid Prototyping Journal*, DOI : 10.1108/RPJ-04-2020-0086, 2021 (to be published).
- [2] Y. Ueda, H. Murakawa, N. Ma. *Welding Deformation and Residual Stress Prevention*. Elsevier, 2013.
- [3] M.Balaa, S.Mekhiel, M.Elbestawi, J.McIsaac, On selective laser melting of Inconel 718: Densification, surface roughness, and residual stresses, *Materials and Design*, Vol : 193, 108818, 2020.
- [4] Q.Chen, X.Liang, D.Hayduke, J.Liu, L.Cheng, J.Oskin, R.Whitmore, A.C. To, An inherent strain based multi-scale modeling framework for simulating part-scale residual deformation for direct metal laser sintering, *Additive Manufacturing*, Vol : 28, 406-418, 2019.



# INNOVATIVE MEASUREMENT METHOD FOR BALANCE PLATFORMS

**E. FROMAGEOT - J. DE CHEVRON VILLETTE**  
**B. DENIS**

# Innovative measurement method for balance platforms

Etienne Fromageot<sup>\*</sup>, Jacques de Chevron Villette<sup>†</sup>, Bruno Denis<sup>◇</sup>

<sup>\*</sup>Département de Génie Mécanique  
Ecole Normale Supérieure Paris-Saclay  
4 avenue des sciences, 91190 Gif-sur-Yvette

Lurpa  
Ecole Normale Supérieure Paris Saclay  
4 avenue des sciences, 91190 Gif-sur Yvette

<sup>\*</sup> [etienne.fromageot@ens-paris-saclay.fr](mailto:etienne.fromageot@ens-paris-saclay.fr)

<sup>◇</sup> [bruno.denis@ens-paris-saclay.fr](mailto:bruno.denis@ens-paris-saclay.fr)

<sup>†</sup> [jacques.de\\_chevron-villette@ens-paris-saclay.fr](mailto:jacques.de_chevron-villette@ens-paris-saclay.fr)

**KEYWORDS:** Stabilometry; measurement; longitudinal balance monitoring, uncertainties, Monte Carlo, numerical simulation.

## ABSTRACT

### General Information

In recent years, life expectancy has increased as never before. It has triggered a new issue concerning the health of the elderly. Studies have shown that it is better for them to live at their own home than at retirement homes [1]. Thus, reliable systems must be designed to monitor the health of these elderly and their ability to remain at home or not. Given that balance is a key indicator, stabilometric platforms have been created to help doctors in their medical follow up. Nonetheless, high-precision platforms are too expensive to be installed in the patient's home, which means that research must be carried out to reduce the cost of platforms reliability. The aim of this study is to develop an innovative mechanical measurement process enabling to identify and quantify the reliability of a stabilometric platform.

### Methods

Quantifying the stability of a person with a platform is commonly achieved by studying the projection of its center of mass (PCM). The aim of this study is to evaluate the measurement uncertainties of the coordinates of the PCM. A first step consists in modelling the behavior of the platform and to quantify the individual uncertainties of the parameters of this model. The propagation will give the measurand uncertainty.

To propagate uncertainties, we used the *Guide to the expression of uncertainty in measurement* (GUM) which serves as an international reference [2]. The main described method is named : the derivative approach. It is based on the computation of first order derivatives of each parameter. It requires mathematical skills which can be very complex depending on the mathematical model.

In view of our model, we decided to use an alternative approach called the method of Monte Carlo which is also authorized by the GUM [3]. In contrast to the derivative approach, this is a numerical technique. It is based on a large number of simulated measurements. The individual uncertainty of each parameter is used to obtain their probability density function : Gaussian distribution for normally distributed data for instance. We draw each parameter according to its probability of occurrence, which we then implement in the model. By making a consequent number of simulations, we obtain a distribution of the output data: its standard deviation will be the measurand uncertainty.

An experimentation was carried out to verify the relevance of the uncertainties determined by the method of Monte Carlo. Measurements of a standard mass allows indeed to compare the measure of the mass with a reference. In the same way, a multi-hole plate with a centering device allows to compare the measure of the PCM with a reference too.

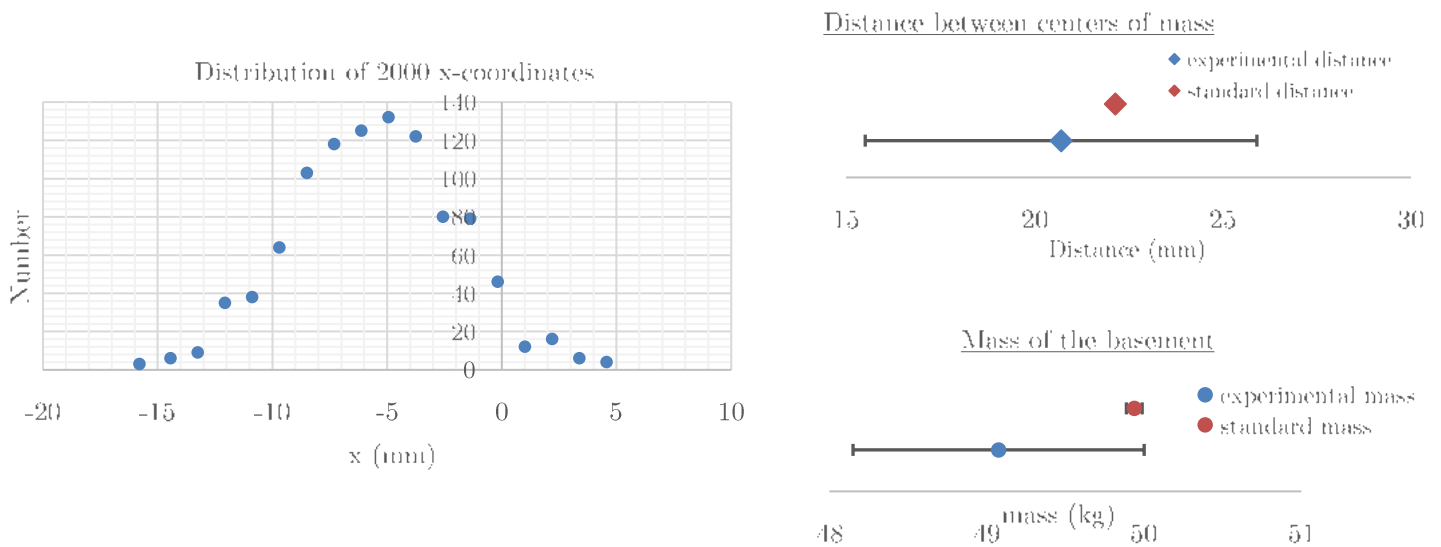
## Results

A first result is the choice of the model for the platform. A first approximation is a linear relation between the force and the digital output to represent each sensor. The force being as well linear with the mass, the model of the sensors chosen links the input (mass) with the output (digit number) with a gain and an offset.

$$\left\{ \begin{array}{l} M = \sum_{i \in A} \frac{Z_i - b_i}{G_i} - m_p \\ x = \frac{\left( \sum_{i \in A} \left( \frac{Z_i - b_i}{G_i} \right) x_i \right) - m_p x_p}{\left( \sum_{i \in A} \frac{Z_i - b_i}{G_i} \right) - m_p} \\ y = \frac{\left( \sum_{i \in A} \left( \frac{Z_i - b_i}{G_i} \right) y_i \right) - m_p y_p}{\left( \sum_{i \in A} \frac{Z_i - b_i}{G_i} \right) - m_p} \end{array} \right. \quad \text{with}$$

- $A = \{SW, SE, NE, NW\}$
- $(x_i, y_i)$  the coordinates of captors
- $(x_p, y_p)$  the coordinates of the center of mass of the platform
- $m_p$  the mass of the platform
- $Z_i$  digital output
- $G_i$  sensor gain
- $b_i$  sensor offsets

As described above, the Monte Carlo method give in output a distribution of the measurand which depends on the individual distributions of the parameters and inputs. After 2000 simulations of measurements, the distribution of the measurand  $x$  obtained is the following one :

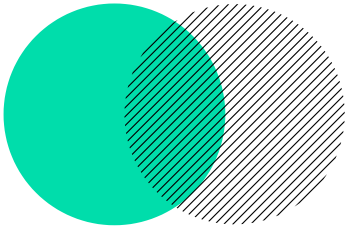


The standard deviation of the distribution gave a large uncertainty especially concerning distances. These uncertainties cover the reference which seems to validate the method. However, the measurement protocol needs to be improved to reduce the distance uncertainty.

It is important to notice that the static behavior considered here has no reason to be the same in dynamics. It could be a relevant idea to use the same method to identify the dynamic response of this stabilometric platform.

## REFERENCES

- [1] D.Maatar, *Analyse des signaux stabilométriques et de la stabilité chez l'Homme : application à la biométrie*. Université Paris-Est, 2013. Français.
- [2] JCGM *Evaluation of measurement data – Guide to the expression of uncertainty in measurement*. First edition September 2008
- [3] Gina Chew, Thomas WALczyk, *A Monte Carlo approach for estimating measurement uncertainty using standard spreadsheet software*



# NUMERICAL STUDY ON THE EFFECT OF THE ROUGHNESS ON THE PHENOMENON OF LOCALIZATION IN POLYCRYSTAL

---

**B. GEORGETTE - E. GERARD**  
**Y. GUILHEM**

TER M1 2020-2021  
9 Mars 2021, Gif-Sur-Yvette, France

école —————  
normale —————  
supérieure —————  
paris – saclay ———

# Numerical study on the effect of the roughness on the phenomenon of localization in polycrystal

B. Georgette\*, E. Gérard†, Y. Guilhem◇

Department of Mechanical Engineering  
Ecole Normale Supérieure Paris-Saclay  
4, avenue des sciences, 91190 Gif-sur-Yvette, France  
e-mail: \* benjamin.georgette@ens-paris-saclay.fr ; † esther.gerard@ens-paris-saclay.fr  
◇ yoann.guilhem@ens-paris-saclay.fr

**KEYWORDS:** microstructure; plasticity; fracture mechanics; finite element analysis.

## ABSTRACT

This study was motivated by the thermodynamical fatigue occurring in the mixing zones of power plant cooling systems. Very short cracks have been observed, having the length of a few grains composing the microstructure. So, the dimensions of the cracks shed light on the microstructure, and its effects on how microcracks appear. To model a microstructure, Schmid law is a precise and easy-to-use tool, which predicts the location and direction of the slippage. Nevertheless, when the surface state presents asperities, there is a competition between microstructure influence (through the Schmid law) and roughness influence on the localization of constraints. The aim of this study is to quantify the comparative influence of microstructure and roughness under uniaxial tensile test on the localization in polycrystals numerically. Previous works have shown first results about the impact of the intensity of the roughness. These results will be completed and the influence of other roughness relative parameters will be studied.

## 1 Methods

A plasticity model is required to compute the behaviour of the microstructure. Méric-Cailletaud's [1] model has been chosen. It indeed shows precise results, and is an easy to use model.

A numerical approach was preferred over an experimental one. Computation has strong advantages, such as costing a considerably short time (when compared to an experimentation), and allowing a control of any parameter. Microstructure is generated with a Voronoï process, generating a Representative Volume Element (RVE), on which the roughness pattern is applied. This pattern is a theoretical one, chosen to be representative of a machined surface. So, a sinusoidal pattern has been selected, since it is easy to monitor its parameters.

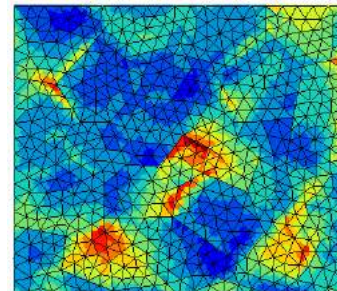


**Figure 1:** Map of the cumulative slip obtained with Zset

These ones are the intensity (represents the depth of the striae), the wavelength (depends on the machining tool), the dephasing between the roughness pattern and thow microstructure is set. Then, the solution in terms of constraints, deformation and cumulated slip are

calculated through a finite elements algorithm resolution. This calculation is based on the plasticity model presented above.

The results given thanks to this process are either maps of the different fields, or tables of values.

## 2 Analysis and first results

Previous studies have based their post-treatment analysis of on the calculation of scalar indicators, named IRPI and IMPI. These are averages of the relative gap between the values of scalar fields with and without roughness or microstructure. These indicators are useful to indicate tendencies, and are easy to use, giving scalar values. However, they are not really satisfying, causing problems when some factors are near to zero.

This study focuses on a different view. The main goal of the post-treatment of data is to identify which parameter has a more significant impact on mechanical behaviour of our RVE. Because of the plurality of results given by our numerical approach, and of how random local results are, through the action of the microstructure, taking a statistical point of view was a rather obvious choice. Then, a statistical method taking into account interactions between various settings was required. This is why Principal Component Analysis (PCA) has been selected [2]. PCA is a statistical method, in which numerous variable fields are observed in the RVE.

Then, the multi-variable space is reduced to a smaller one, whose axes are composed of a linear combination of previous fields. This data reduction analysis highlights which variables prevail in the behaviour of an RVE. By performing PCA on various RVE, with different settings, it is possible to observe the impact of these parameters on how mechanical fields behave.

The first results of our simulation confirm demonstration of previous papers about the influence of the intensity of roughness, and allow us to identify laws about the influence of the dephasing.

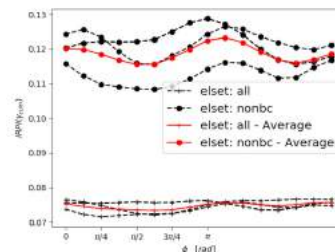
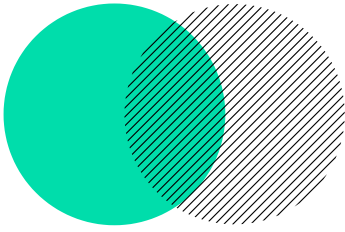


**Figure 2:** Sinusoidal variation of the IRPI with the dephasing

## REFERENCES

- [1] Stéphanie Basseville, Georges Cailletaud, T. Ghidossi, Yoann Guilhem, E. Lacoste, et al.. Numerical analysis on the local mechanical fields in polycrystalline 316LN stainless steel under cyclic fatigue loading: Comparison with experimental results. *HAL* Vol:696, pp.122-136, 2017.
- [2] Zulaikha Geer. Understanding Principal Component Analysis (PCA). *AI Zone* 2019



# STABILOMETRY PLATFORM FOR BALANCE CHARACTERIZATION

---

**A. BEAUQUEL - B. HAMEL**  
**G. FARAUT**

TER M1 2020-2021  
FINAL DEFENSE OF RESEARCH PROJECTS  
13 April 2021, Gif-Sur-Yvette, France

école —————  
normale —————  
supérieure —————  
paris – saclay ———

# Stabilometry platform for balance characterization

Antoine Beauquel, Baptiste Hamel, Gregory Faraut \*

\* Department of Mechanical Engineering  
University Paris-Saclay - École Normale Supérieure Paris-Saclay  
4 Avenue des Sciences, 91190, GIF SUR YVETTE  
e-mail: antoine.beauquel@ens-paris-saclay.fr, baptiste.hamel@ens-paris-saclay.fr

**KEYWORDS:** Statokinesigram, Classification method, Machine learning.

## ABSTRACT

### Introduction

Elder people could develop balance troubles which can lead to a fall, and then to injuries. To avoid this situation, their balance can be controlled by doctors whereas it involves a regular follow-up of patients which is restrictive and not so regular. To analyse the behavior of the balance, specialists can use a platform to analyse the position of the center of pressure depending on time while the patient tries to stay static. The literatures pinpoints that specialists have difficulties to analyses datas provided by the system, so developers chosed to attribute a score to qualify the balance [1][2].

The aim of this study is to develop a similar household device to let patients evaluate more regularly their balance. The balance quality tester (BQT) is then used in less controled conditions than when they are realized by a specialist. The BQT is made up of a platform which rests on 4 load cells, what allows to measure the vertical resultant in each sensor to deduce the movement of the projection of the preasure center. The graph obtained is called SKG.

### 1 Criteria to evaluate balance

We characterized each SKG using different methods : already existing methods were used [1], and we developed new ones. The Takagi's ellipse [3], which is the smallest ellipse containing 90% of the points of the SKG was implemented to describe the SKG with the area, or the size of the two axis of the ellipse. We also calculated the average speed of the norm and along medio-lateral and anterior-posterio axis. As new criteria, we defined the average speed of remoteness and the average speed of rapprochement. We defined those criteria as the norm of the speed vector when it is pointing at the direction of the center of the Ellipse or to the opposite with an adjustable margin. Because of the duration of an experiment is enough short, we state the hypothesis that the center does not change.

### 2 Patient classification based on previously defined criteria

To determine a patient's possible illness, the following formalism was used: Individuals are grouped into belonging classes according to their pathologies and how the SKG was registered. To determine the class of an individual the method of the k-nearest neighbors (KNN) was used [4]. We place ourselves in the space  $\mathcal{R}^n$  formed by the data of  $n$  criterion chosen from the criteria described above. This space is associated with a weighted norm 2 for each component. The class of the unknown individual is interpolated as the majority class among its k-nearest neighbors as described on figure 1. The distance is calculated with the weighted norm 2 (Euclidean norm) for each component.

### 3 Test and improvement of the classification

To test the KNN method, we constitute two data bases from two experimental campaigns. In the first one, patients were tested two times during one minute, standing on their two legs with opened and then closed eyes, while in the

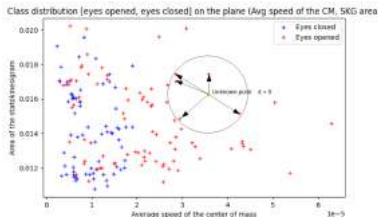


**Figure 1:** Diagramm of the k-nearest neighbors method in our case

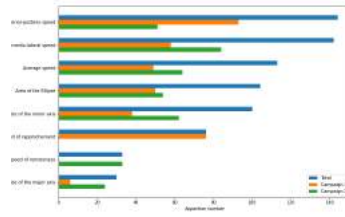


**Figure 2:** Number of apparitions of criteria among the best 100 distributions

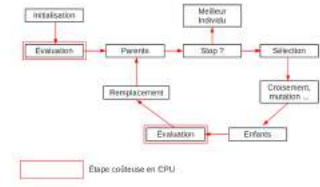


**Figure 3:** Diagram of the genetic optimization algorithm

second, they are tested 4 times, standing on one leg with opened and then closed eyes. As a proof of concept, we decided to study the following classification : [opened eyes, closed eyes].

We first try to determine for each database which criteria and which value of K were the most relevant to classify people. To do this, we evaluated the average percentage of success and the standard deviation when we tested the algorithm on random test data extracted from data bases. We reached 63,2% and 100% of successful classification for respective campaigns what pinpoints that classification method could be used. Figure 2 shows how relevant are the criteria in the two study : those which were developed seem to be pertinents.

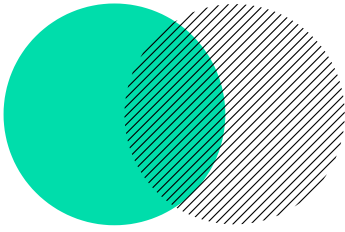
In order to guarantee a calculation of the distance which allows a good classification, a work on the weighted Euclidean norm had to be undertaken. Some criteria make it possible to be more differentiating than others when classifying. These criteria must be put forward in the calculation of the distance, the others will be allocated a lower weighting. To find the right set of parameters for weighting in the Euclidean norm, a genetic optimization algorithm has been developed [5]: Each weighting coefficient is coded on a 16-bit gene, a genome being composed of as many genes as there are criteria used in k-NN algorithm. The associated fitness function is chosen as the average of the good classification pass percentage for several trials with a different reference population minus the standard deviation of this distribution. The son genes are generated by assembling the first and last parent gene halves, then one or more randomly selected bits are exchanged to create genetic diversity through mutations.

## Conclusion

In the course of our study, we were able to define and calculate new criteria for assessing balance by reading a statokinesigram. These new criteria are in addition to other criteria already developed in the literature. Various test campaigns have been carried out to build a sufficiently strong database of 296 recordings. A proof of concept of patient classification by k-NN algorithm was also implemented. This has required work to optimise the criteria used and the weighting given to them, work which was carried out in the last part of our study.

## REFERENCES

- [1] G. Sourdain *Stabilométrie statique : Place de la plateforme de force en kinésithérapie*, 2011.
- [2] J. Duchêne, D. Hewson, P. Rumeau *Modified bathroom scale and balance assessment: a comparison with clinical tests*, 2016.
- [3] P.M. Gagey *Calcul de la surface du statokinésigramme (SKG)*. Association Française de Posturologie 1993.
- [4] P. Cunningham, S.J. Delany. *k-Nearest neighbour classifiers*, 2007.
- [5] I. Saad, F. Tangour, P. Borne. *Application des algorithmes génétiques aux problèmes d'optimisation*. Revue de l'électricité et de l'électronique, 2009.



# INTERPOLATION AND FILTERING TRAJECTORIES FOR LASER POWDER BED FUSION ADDITIVE MANUFACTURING

---

**M. EL HOUZI - A. GEFFRELOT**  
**K. GODINEAU**

TER M1 2020-2021  
FINAL DEFENSE OF RESEARCH PROJECTS  
13 April 2021, Gif-Sur-Yvette, France

école —————  
normale —————  
supérieure —————  
paris — saclay —————

# Interpolation and filtering trajectories for laser powder bed fusion additive manufacturing

Mohamed-Amine EL HOUZI\*, Alexis GEFFRELOT†, Kevin GODINEAU◇

\* † Département de Génie Mécanique  
École Normale Supérieure Paris-Saclay  
4, rue Yvette Cauchois  
91190 Gif-sur-Yvette, FRANCE

\* e-mail: mohamed-amine.el\_houzi@ens-paris-saclay.fr

† e-mail: alexis.geffrelot@ens-paris-saclay.fr

◇ LURPA, Laboratoire Universitaire de Recherche en Production Automatisée

École Normale Supérieure Paris-Saclay  
4, rue Yvette Cauchois  
91190 Gif-sur-Yvette, FRANCE

e-mail: kevin.godineau@ens-paris-saclay.fr

**KEYWORDS:** Laser powder bed fusion process ; Filtering ; Contour error.

# ABSTRACT

## General Information

Laser powder bed fusion additive manufacturing machines restrict capacities of the process owing to the limited dynamic of actuators. In order to smoothen these commanded velocities, the displacement, velocity or acceleration will be filtered with a finite impulse response filter (FIR) [2](figure: 1). In filtering with a first order FIR filter, which is a rectangular window function, it will limit the acceleration, however, initial trajectories will be approximated in corners, which will lead to contour errors. To the best of our knowledge, no previous work has already created a filter minimising the contour error in relation to the reference trajectory while keeping the commanded velocity. Thus, the aim of this study is to develop such a filter arrangement.

## Methods

To design this filter, First, we chose to filter the position of the laser spot and bring the dynamic limits of actuators to the task space as a dynamic constraints on a x and y movements, that we consider constant as a function of the task space, and which is worth the minimum that corresponds to the dynamic limits at the centre of the task space. Thereby, we will study a corner between two segments configured with an angle  $\theta$  and traveled with a constant speed. We studied a filter with a negative part as defined in the figure: 1. It allows us to limit the system's dynamic and minimise the error between the filtered trajectory and the setpoint, it allows us also to create a under-corner and over-corner trajectory [1]. This filter is set by three parameters, and the last one is fixed by the area of the filter. When this filter modify the trajectory, it creates a part out of material and a part in the material so it creates, in comparison with the top-hat filter, tow different cord errors but still smaller than the cord error if the top hat filter. About the velocity, we demonstrate that the decrease of the speed is independent of the filter used.

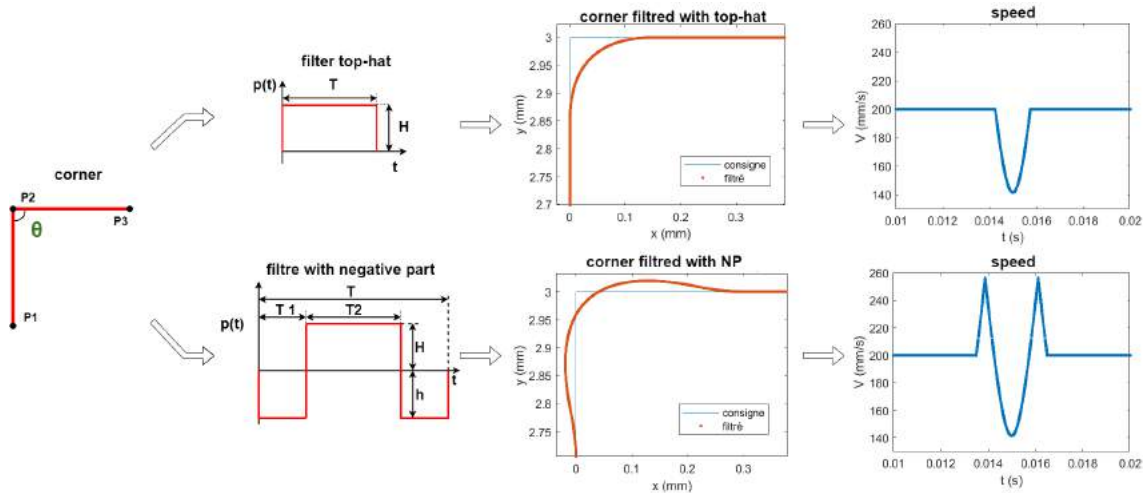
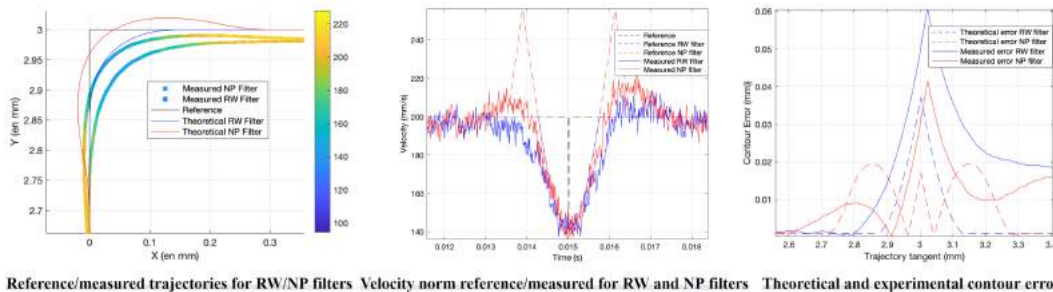


Figure 1: Filtering operation for both FIR filters

## Results

For the purpose of confirming our mathematical relations and numeric simulation, an experiment has been conducted with an instrumented test bench. From a reference trajectory, it has been filtered with a FIR top hat (TH) 1 and FIR negative part (NP)1 filter. Then, data have been converted into articular references by using an inverse cinematic model in order to send it to machine's controlling system.



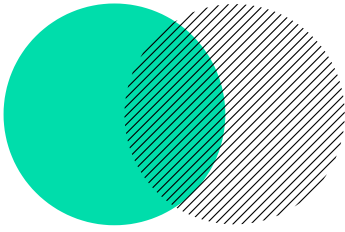
On the one hand, our results show that the NP filter generates less contour errors in comparison with the signal observed for the TH filter. According to our measures for the corner studied Figure , contour errors, concerning the NP filter, are respectively, 31,4%, 27,4% and 26,3% lower than errors generated with a TH filter. Moreover, the NP filtered trajectory offers the most geometrically accurate contouring motion of the reference trajectory in regard to the TH filtered trajectory according to Figure . Thanks to the undercorner and overcorner trajectory [1] with the NP filter, it allows the laser dot to come closer nearer to the corner. On the other hand, the use of NP filter introduces higher speed skip which are more restrictive for actuators, according to Figure . The overcorner displacement of the laser dot impacts the norm of velocity with higher values and then will lead to further up acceleration than with a TH filter.

## Conclusion

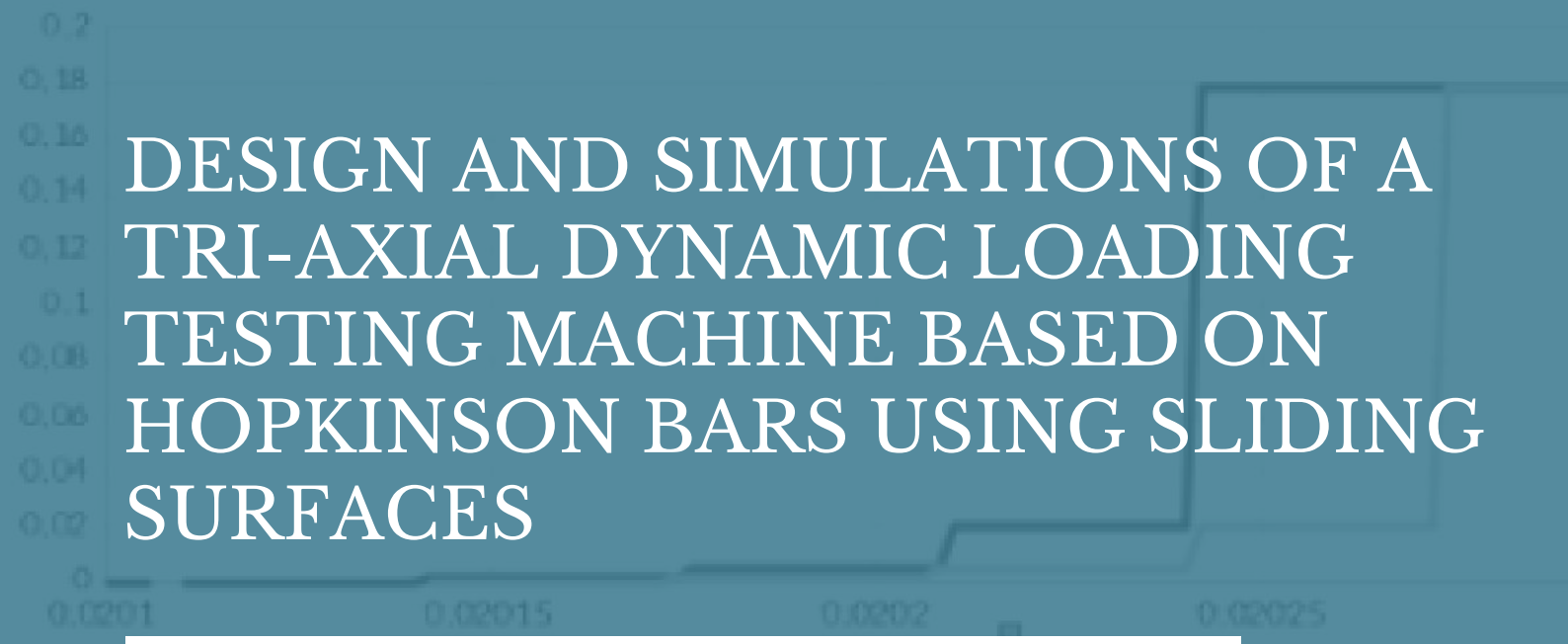
In our study, a new filter has been configured and the cord error has been calculated between the filtered trajectory and the setpoint. Then, the NP filter has been optimized to get the minimum of the cord error in a corner and allowing the laser dot to do undercorner and overcorner trajectories. Finally, this work shows that the velocity decrease in corners is constant and not related to the type of filters used. Further studies would be conducted on the impact of FIR NP filters on the local deposited energy in corners.

## REFERENCES

- [1] Kaan Erkorkmaz, Chi-Ho Yeung, and Yusuf Altintas. Virtual cnc system. part ii. high speed contouring application. *International Journal of Machine Tools and Manufacture*, 46(10):1124–1138, 2006.
- [2] Shingo Tajima, Burak Sencer, and Eiji Shamoto. Accurate interpolation of machining tool-paths based on fir filtering. *Precision Engineering*, 52:332–344, 2018.

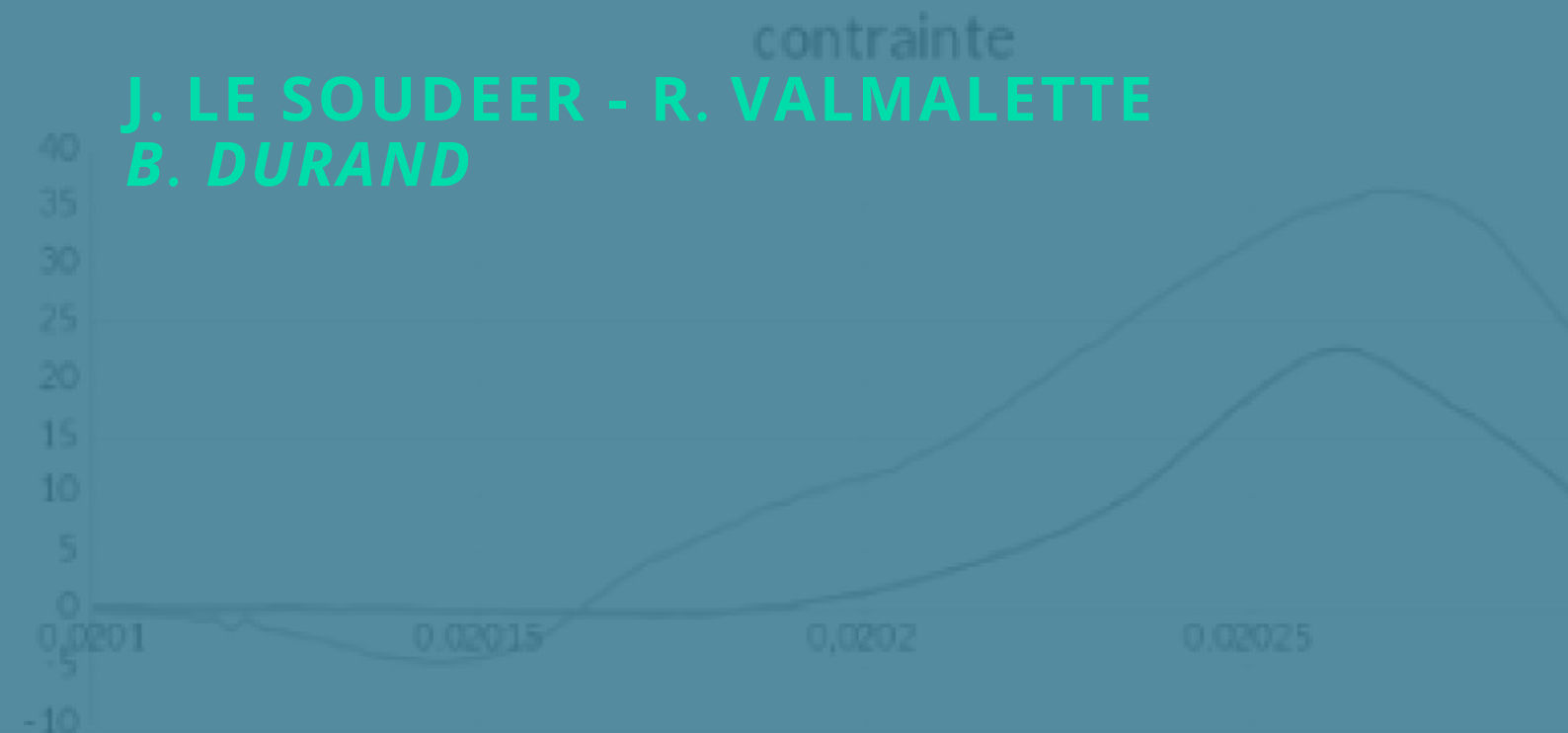


deformation camera



# DESIGN AND SIMULATIONS OF A TRI-AXIAL DYNAMIC LOADING TESTING MACHINE BASED ON HOPKINSON BARS USING SLIDING SURFACES

contrainte



**J. LE SOUDEER - R. VALMALETTE**  
**B. DURAND**

TER M1 2020-2021  
FINAL DEFENSE OF RESEARCH PROJECTS  
13 April 2021, Gif-Sur-Yvette, France

école \_\_\_\_\_  
normale \_\_\_\_\_  
supérieure \_\_\_\_\_  
paris-saclay \_\_\_\_\_

# Design and simulations of a tri-axial dynamic loading testing machine based on Hopkinson bars using sliding surfaces

Jeanne Le Soudeer\*, Robin Valmalette<sup>†</sup>, Bastien Durand<sup>◇</sup>

\* <sup>†</sup> Department of Mechanical Engineering  
Ecole Normale Supérieure Paris-Saclay  
4 avenue des Sciences, 91190 Gif-sur-Yvette  
\* e-mail: jeanne.le\_soudeer@ens-paris-saclay.fr  
<sup>†</sup> e-mail: robin.valmalette@ens-paris-saclay.fr

<sup>◇</sup> LMT  
ENS Paris Saclay  
e-mail: bastien.durand@ens-paris-saclay.fr

**KEYWORDS:** Triaxial compression dynamic test; Hopkinson bars; finite element simulations (dynamic explicit).

## ABSTRACT

### General Information

Dynamic stresses inside materials are massively present in many fields like automotive or high-speed machining. Therefore, understanding the behavior of the materials allows engineers to design properly mechanisms. Most of the time, multi-axial loading occurs whereas most of experimental devices study materials with uni-axial loading. Moreover, the behavior of the material is related to many factors such as axes of loading, the speed of loading and the type of stress: tension or compression.

In order to perform multi axial loading, several set-ups have been designed such as a rigid cylinder to confine a cylindrical sample. In this example the sample is radially loaded by Poisson's effect [1].

None of such existing systems answer to the need of a uniform triaxial loading independent from the material properties and sample shape. The aim of this study is to design and simulate such a device. It is based on the method of Hopkinson bars which originally can not generate synchronous loading.

### Methods

The chosen technology uses sliding surfaces to transmit a dynamic loading from a striker to loading bars in three perpendicular directions. The architecture of this device is shown in figure 1. It is a combination of the biaxial Hopkinson bars described in [2] and a third axis. The third axis is loaded via two beveled edges, like the two other axis, at an angle of 45°. The mechanism is built with the right dimensions to suppose a uniaxial propagation of the wave in the loading bars. Two gauges are placed on each loading bar to assess the displacement due to the loading and the sample reaction. A Lagrange diagram figure 2 is used to analyse such collected data. The same method of analysis is applied on the biaxial

and triaxial models.

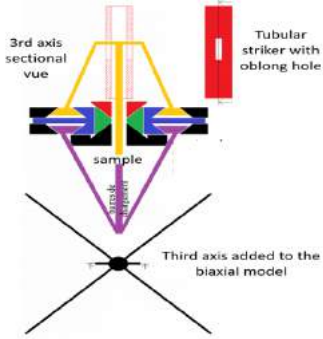


**Figure 1:** Architecture of the triaxial Hopkinson bar device

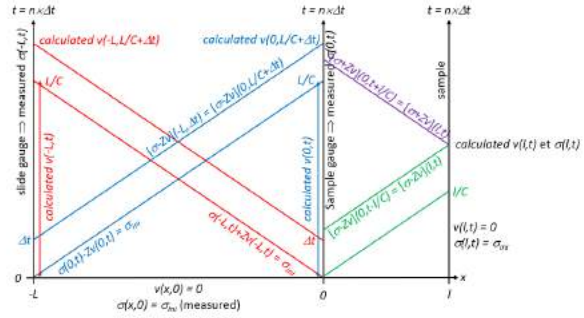


**Figure 2:** Lagrange diagram for data analysis

To confirm the results and to properly design the system, a numerical model is built on Abaqus software. A triaxial model was built in addition to the already existing biaxial model. The strain can be collected on any element of the meshed loading bars, especially where the gauge would be placed. The Lagrange diagram and equations can be used in the same way experimentally and numerically.

## Results

Given the positions of the strain gauges, the simulation gives results (see 3) which fit, in both cases of boundaries, with the simulation at the interface with the input bar and the specimen. This simulation allowed us to chose the best position for the strain gauges to respect Saint-Venant conditions and avoid inhomogenous wave propagation in the studied section. The experimental device is left to be built.

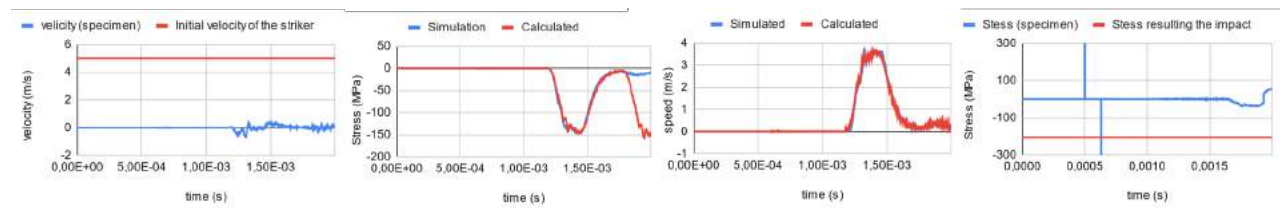
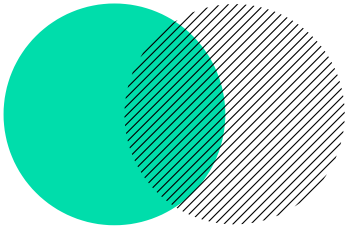


**Figure 3:** Stress and velocity in the case of a blocked boundary (left) and of a free boundary (right)

## REFERENCES

- [1] W. Chen, B. Song. Split Hopkinson (Kolsky) Bar. Design, Testing and Applications. 422 Springer Science Business Media, LLC (2011)
- [2] B. Durand, P. Quillery, A. Zouari, H. Zhao, Exploratory tests on a biaxial compression Hopkinson bar set-up (2021), 10.1007/s11340-020-00665-7



# DESIGN AND VALIDATION OF MESO-STRUCTURES FOR THE MANUFACTURING OF A PHYSICAL TWIN OF SKIN IN MULTI-MATERIAL 3D PRINTING

---

**A. LAGACHE - V. MAGGIONI**  
**F. DAGHIA**

TER M1 2020-2021  
FINAL DEFENSE OF RESEARCH PROJECTS  
13 April 2021, Gif-Sur-Yvette, France

école —————  
normale —————  
supérieure —————  
paris – saclay ———

# TER - Design and validation of meso-structures for the manufacturing of a physical twin of skin in multi-material 3D printing

Alexandre Lagache\*, Valentin Maggioni\*, Federica Daghia $\diamond$

\* Département de génie mécanique  
École normale supérieure Paris-Saclay  
4 Avenue des Sciences, 91190 Gif-sur-Yvette  
e-mail: {alexandre.lagache,valentin.maggioni}@ens-paris-saclay.fr

$\diamond$  Université Paris-Saclay, ENS Paris-Saclay, CNRS  
LMT - Laboratoire de Mécanique et Technologie  
4 Avenue des Sciences, 91190 Gif-sur-Yvette  
e-mail: federica.daghia@ens-paris-saclay.fr

**KEYWORDS:** Meso-Structure; Biomechanics; Finite Element Simulation.

## ABSTRACT

This study aims to develop a human skin mimic using 3D multi-material printing techniques, that will be used as atask trainer for surgeons in training. In particular, it focused on studying skin for the surgical operation of cricothyroidotomy, a first aid method used to help patients with obstructed airways. This project is the continuation of a previous study carried out last year by A. Burak Irez in collaboration with Biomodex and the LMT at ENS-Paris-Saclay [1].

In order to achieve this goal, we focused on three axes. Firstly, we studied A. Burak Irez's paper and tried to develop simple analytical models to estimate the property of the materials. We then focused on the differences between Burak Irez's experimental and numerical results. Secondly, we developed our own numerical models and proceeded to an experimental phase. Finally, we studied our results and proposed new methods to mimic human skin.

As such, our first approach was to create an analytical and simplified bi-linear model of the material designed by Burak Irez and printed by Biomodex. The material he designed was a composite material made of a soft and elastic matrix containing a set of undulated stiff fibers. This bi-linear model was inspired by the literary review of another study [2] and presented a simplified way of foreseeing the results of a tensile test on the designed material.

We then compared the analytical model to the numerous numerical simulations and the experimental results that he had obtained during his study.

This comparison highlighted several differences between these models, such as the inability of the fibers to realign themselves completely and the difference in the maximum load that the fibers could sustain. As such, we emitted various hypothesis to explain these differences, namely regarding the stiffness and rigidity of the fibers and the boundary conditions used for the numerical simulations.

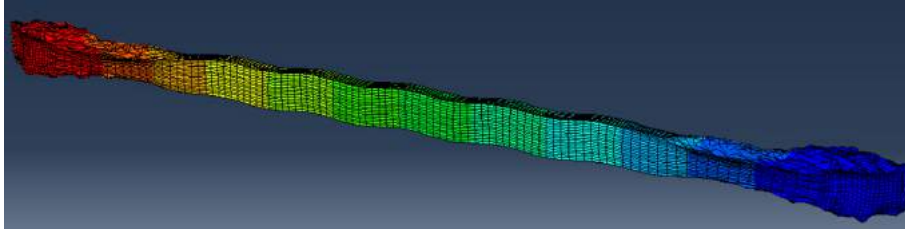


**Figure 1:** Finite elements simulation with modified boundary conditions

In order to verify these hypothesis, we designed various numerical studies and experimental campaigns to refine the previous material design. For that purpose, we designed two new numerical models using the finite element method. The first model redefined the boundary conditions of the Burak Irez’s initial model to fit with the experimental conditions (see Figure 1). The second model applied the same material as the fiber on the tips of the test-piece in order to help the fibers unfold.

We were then given several test pieces of the material by Biomodex in order to perform new tensile tests. The experiments we conducted allowed us to see the behaviour of the material until its rupture. We photographed the test-pieces during the whole experiments in order to examine the unfolding of the fibers throughout the tensile test. As a result, we were observed that while the fibers had yet to unfold completely during the test, even with the new materials.

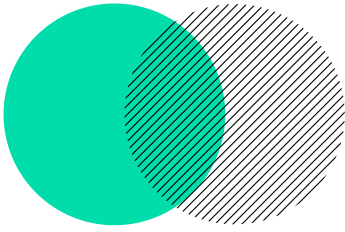
The results following this study led us to consider new mesoscopic models for the material. In order to verify the validity of these models, we performed a second experimental campaign using microscopic observations to observe the fibers inside the matrix and the interface between the matrix and the fibers. These observations gave us new insight on what happened to the fibers during the previous experimental campaign.

Those experiments helped us to understand several phenomenons we initially neglected, like the elasticity of the fiber. This elasticity prevents the fibers from unfolding as predicted. Furthermore we identified several other parameters that can influence the unfolding of the fibers, such as the elasticity modulus of the fibers. Finally our analysis revealed that a third material is likely to be at the interface between the fibers and the matrix, influencing their elastic behaviour.

Our results could also pave the way to further investigations. For example, the study of the material with elasto-plastic fibers may give numerical simulations closer to the experiments than before. However, to achieve the design of a material with skin-like behaviour the chosen materials have to be reconsidered.

## REFERENCES

- [1] A.Burak Irez *Design and development of human skin mimics*. unpublished, 2020.
- [2] J.W.Y. Jor, M.D. Parker, A.J. Taberner, M.P. Nash, P.M.F. Nielsen, Computational and experimental characterization of skin mechanics: identifying current challenges and future directions *Wiley Interdiscip. Rev. Syst. Biol. Med.* **5**:539-556, 2013. <https://doi.org/10.1002/wsbm.1228>.



# TOMOGRAPHIC MONITORING OF A TORSION TEST ON A METAMATERIAL

---

**M. VALMALLE - A. VINTACHE**  
**B. SMANIOTTO - F. HILD**

TER M1 2020-2021  
FINAL DEFENSE OF RESEARCH PROJECTS  
13 April 2021, Gif-Sur-Yvette, France

école \_\_\_\_\_  
normale \_\_\_\_\_  
supérieure \_\_\_\_\_  
paris-saclay \_\_\_\_\_

# Tomographic Monitoring of a Torsion Test on a Metamaterial

M. Valmalle\*, A. Vintache\*, B. Smaniotto\*,<sup>◇</sup>, F. Hild<sup>◇</sup>

École normale supérieure Paris-Saclay  
4 avenue des Sciences, 91190 Gif-sur-Yvette, France  
e-mail:{malo.valmalle,antoine.vintache,benjamin.smaniotto,  
francois.hild}@ens-paris-saclay.fr

\* Department of Mechanical Engineering  
<sup>◇</sup>LMT - Laboratoire de Mécanique et Technologie

**KEYWORDS:** Digital Volume Correlation; Pivot; Tomography; Torsion Test.

## ABSTRACT

Pantographic metamaterials are known for their peculiar mechanical properties [1]. However, few studies were conducted on twisted 3D printed pantographs. This project aims at performing an in situ torsion test on a pantograph made of titanium alloy in an X-ray tomograph. The acquired scans were used to measure displacement fields via digital volume correlation. The final goal is to analyze the fracture and deformation mechanisms of the tested metamaterial.

## Methods

The torsion test was monitored using micro-computed tomography. This imaging technique is nondestructive and provides 3D images of the sample. The torsion torque was applied by two angular actuators of the in situ testing machine, both controlled in angular position. The levels of torque and axial force were regularly recorded. The test was conducted until complete fracture of the pantograph at an angular amplitude of  $90^\circ$  between the bottom and top grips (Figure 1).

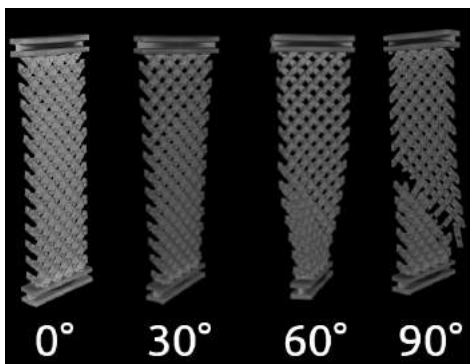


**Figure 1:** 3D renderings of the tested sample for different angular amplitudes  $\theta$  in torsion

The volume size was  $49.6 \times 49.9 \times 91.6 \text{ mm}^3$  with a  $66 \mu\text{m}$  per voxel resolution. The series of radiographs (i.e. sinograms) were used to reconstruct 3D images of the sample (Figure 1). The displacement fields were then measured using Digital Volume Correlation (DVC). Two different meshes were used, a coarse one for the initialization of DVC and a fine one for the actual calculations (Figure 2).

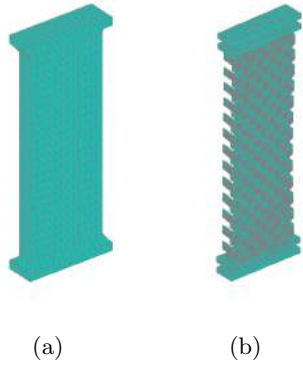


**Figure 2:** Coarse (a) and fine (b) meshes used for DVC analyses

Due to the large deformations between each angular amplitude during the test, the DVC calculations had to be properly initialized. A digital image correlation algorithm was used on each nodal plane of the coarse mesh (Figure 2(a)) allowing only rigid body motions to be measured. The nominal geometry (i.e. the mesh) was also backtracked on the experimental reference configuration in order to ensure that it lied in the reference configuration of the test. DVC was then run on the first two deformed configurations (Figure 1) with mechanical regularization [2] using the fine mesh (Figure 2(b)). To account for the 234 pivots, multi point constraints were implemented by penalizing mean displacement jumps for each pivot in order to minimize the interpenetration of the different parts (i.e. pivots and beams) of the pantograph.

## Results

Even with such large deformations between the analyzed volumes (Figure 1), the DVC calculations converged thanks to the implemented initialization, backtracking procedure and two regularization strategies. The displacement field in the out-of-plane (i.e.  $y$ ) direction (Figure 3(a)) has a range of  $\pm 120$  voxels for an angular amplitude of  $60^\circ$ . Such a range validates the use of the previously cited methods to allow DVC calculations to converge. The maximum principal strain  $\epsilon_1$  field (Figure 3(b)) for the same angular amplitude highlights the onset of fracture that was observed experimentally (Figure 1). There is a clear concentration of  $\epsilon_1$  on the pivots and beams near what became the fractured zone.

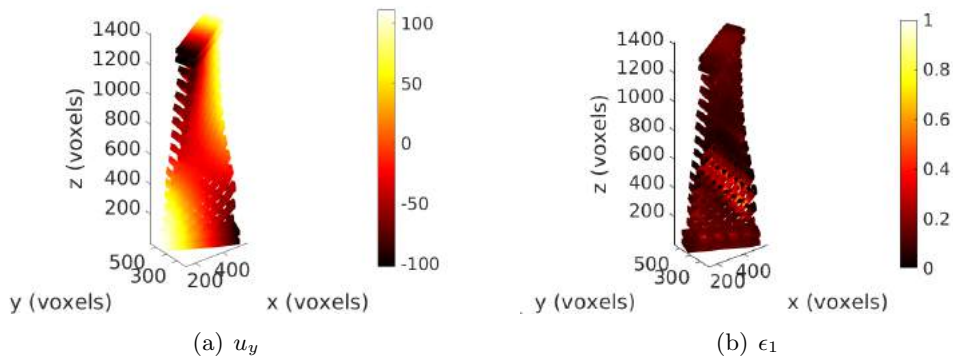


**Figure 3:** Displacement field  $u_y$  (expressed in voxels, 1 voxel  $\equiv$  66  $\mu\text{m}$ ) and maximum principal strain  $\epsilon_1$  for an angular amplitude of  $60^\circ$

## REFERENCES

- [1] A. Misra, T. Lekszycki, I. Giorgio, G. Ganzosch, W.H. Müller, and F. dell’Isola. Pantographic meta-materials show atypical poyniting effect reversal. *Mech. Res. Comm.*, 89:6–10, 2018.
- [2] T. Taillandier-Thomas, S. Roux, T.F. Morgeneyer, and F. Hild. Localized strain field measurement on laminography data with mechanical regularization. *Nucl. Inst. Meth. Phys. Res. B*, 324:70–79, 2014.